Supplemental Materials

Molecular Biology of the Cell

Pfeifer et al.

Supplemental figure legends

Figure S1. Tomasetti and Vogelstein correlated human cancer risk with DNA replication in all normal tissue stem cells, and the correlation is steeper for the stiffer tissues, which present stiffer obstacles during migration.

(A) (i) Tomasetti and Vogelstein showed that the lifetime cancer risk *R* for a given tissue increases with the lifetime number of stem cell divisions *D* in that tissue [1]. Nowak and Waclaw used a simple mathematical model to predict that *R* should be linearly proportional to *D* in the one-hit (oncogene) initiation case and to D^2/N in the two-hit (tumor suppressor genes) initiation case. *N* is the number of stem cells present in the tissue. However, in each case, the correlation is sub-linear for reasons yet unknown [2]. Plotted data were obtained from [1], and the classification of cancers as either 'deterministic' or 'replicative' was adapted from [2]. (ii) Fitting only the stiffest tissues (red points and line) yields both an improved R^2 value and a slope closer to the expected value of one. These improvements hint at an interaction between tissue stiffness and mutations in replication. Soft tissues and tissues of intermediate stiffness are fit with a dark green line. (iii)Idealized plot illustrating that cancer risk *R* increases with stem cell divisions *D*, as shown above in panels i and ii, and both increase with tissue stiffness [3,4].

(B) As reported in Figure 1B, controlled pressure was applied to A549 cells in which the genomic LMNB1 gene is tagged with a red fluorescent protein. The cells showed loss of LMNB1 at the tip of the nucleus, signaled by a decline over time in the tip-to-outside RFP-LMNB1 intensity ratio. Here, a phenomenological theory of the time-dependent redistribution of lamin-B during constriction predicts how the change in concentration of lamin-B molecules at the nuclear tip varies with pipette radiusR_p. The absolute value of the RFP-LMNB1 intensity ratio slope (Fig. 1B-i,ii) is predicted to decrease with increasing pipette radius such that|slope| is linear in $1/\text{radius}^4$. Data points are taken from Fig. 1B-ii and fit according to the predicted scaling from the phenomenological theory (blue line), which is described in the "Theoretical model for curvature-driven dilational flow of lamin-B" section of Materials and Methods. Inset is a schematic diagram of the deformed shape of the nucleus during aspiration. This deformed shape is roughly divided into three regions: (1) a spherical nuclear region of radius R_n; (2) a cylindrical region of radius R_p; and (3) a tip region, which is a spherical section of radius R_p.

(C) During micropipette aspiration, cells showed dilation of lamin-B and leakage of GFP-53BP1 out of the nucleus without blebbing. Blue dashed line indicates the bounds of the nucleus. (Scale bar is 5 μm.)

Figure S2. For all three cancer cell lines tested, the number of γH2AX foci per DNA decreases in late cell cycle, consistent with cell cycle checkpoints for DNA damage.

(A) Across seven experimental conditions (3 μm/8 μm, top/bottom, 2D low/med/high), the average number of γH2AX foci per total DNA content was calculated for every phase of the cell cycle (G1, eS, lS, G2, M), and then normalized to the the average number of γH2AX foci per DNA in G1. These normalized values were then averaged across all experimental conditions. 'ND' = 'not detected'. (≥ 60 cells per condition, n = 2 experiments, error bars represent SEM.)

(B) Using fluorescence microscopy of Hoechst-stained cells, mitotic spindles were counted for each experimental condition (3 μm/8 μm, top/bottom, 2D low/med/high), and % mitotic was calculated. 'ND' = 'not detected'. (≥ 60 cells per condition, n = 2 experiments, error bars represent SEM.)

Figure S3. Multiple U2OS migration experiments confirm that constricting pores deplete the population of 4N cells and cause excess DNA damage.

(A) In eight separate U2OS Transwell migration experiments, cells were measured for γH2AX foci number and, based on total DNA content, classified as 2N or 4N. Plots show average values of % 4N, γH2AX foci, γH2AX foci per total DNA content in 4N nuclei (relative to γH2AX foci per DNA in 2N nuclei), and cell density. Asterisk indicates a significant difference in % 4N between 3 μm 'Bottom' and 'Top' cells (p = 0.02). (≥ 60 cells per condition, n = 8 experiments, error bars represent SEM.)

(B) (i) For each experimental condition (i.e. 3 μm/8 μm, top/bottom, 2D low/med/high), the average number of γH2AX foci was calculated for every phase of the cell cycle (G1, eS, lS, G2, M), and then normalized to the the average number of γH2AX foci in G1. These normalized values were then averaged across all experimental conditions. (≥ 60 cells per condition, n = 2 experiments, error bars represent SEM.) The same analysis was performed for γH2AX foci in U251 and A549 cells (Fig. 5A) as well as for BRCA1 and 53BP1 foci in U2OS cells. (ii) As described in Fig. 5A, the "predicted" number of BRCA1 and 53BP1 foci

was computed for 3 μm and 8 μm top and bottom. Then, the measured (bottom/top) foci ratio was plotted against the predicted foci ratio. Unlike γH2AX foci, excess BRCA1 foci after constriction can be explained as a consequence of perturbations to the cell cycle distribution. Meanwhile, constricted migration does not cause an increase in 53BP1 foci in U2OS cells.

Figure S4. Partial knockdown of the topoisomerase TOP2A does not eliminate excess DNA damage due to constricted migration.

(A) (i) siRNA was used to partially knock down the topoisomerase TOP2A. Knockdown efficiency was determined by immunofluorescence microscopy. Asterisk indicates that TOP2A intensity is significantly lower in siTOP2A cells than in NT ($p< 1\times10^{-9}$) or siCtrl ($p< 1\times10^{-14}$) cells; TOP2A intensity is slightly but significantly ($p = 0.04$) elevated in siCtrl cells compared to NT. (≥ 120 cells per condition, error bars represent SEM.) (ii) Following 72-hour transfection with siRNA targeting TOP2A, U2OS cells were migrated through 3 μm pores. (iii) If TOP2A were responsible for the excess DNA damage observed after 3 μm pore migration, then siTOP2A cells would be expected to show a smaller increase in γH2AX foci after migration than their wild-type (non-treated or siCtrl) counterparts. However, partial depletion of TOP2A does not strongly affect the excess DNA damage, indicating that the damage is not caused by topoisomerase activity. The asterisk indicates that siTOP2A cells on 'Top' show a small but significant ($p< 0.05$) decrease in γH2AX foci compared to NT or siCtrl cells on 'Top', which is sensible given that topoisomerase is a source of DNA breaks. There is no significant difference in γH2AX foci among any of the 'Bottom' conditions. (≥ 135 cells per condition, n = 2 experiments, error bars represent SEM.)

(B) (i) U2OS cells were migrated through 3 μm pores in the presence of the drug etoposide, which induces DNA damage during S phase. (ii) Etoposide does not affect the rate at which cells migrate through small pores [5], with both 2N and 4N cells migrating (iii). (≥ 75 cells per condition, error bars represent SEM.)

Figure S5. Treatment with PD, a CDK4/6 inhibitor, suppresses DNA synthesis and mitosis, effectively 'freezing' cells in G1 or G2.

(A) After 72-hour treatment with 10 μMPD, U2OS cells show a reduction in S phase, as indicated by EdU incorporation, and mitosis, as indicated by Hoechst-stained mitotic

spindles. Both small (2N) and large (4N) nuclei are observed after PD treatment, suggesting that cells are arrested in either G1 or G2. (≥ 80 cells per condition, n = 3 experiments.)

(B) PD treatment yields a reduced cell density on the top and bottom of the Transwell membrane, as compared to the control condition (Fig. 2C). (≥ 75 cells per condition, n = 2 experiments, error bars represent SEM.)

References

1. Tomasetti C, Vogelstein B: **Variation in cancer risk among tissues can be explained by the number of stem cell divisions**. *Science.* 2015, **347**:78–81.
2. Nowak MA, Waclaw B: **Genes, environment, and "bad luck."***Science.* 2017, **355**:1266–1267.
3. Klein EA, Castagnino P, Kothapalli D, Yin L, Byfield FJ, Xu T, Levental I, Hawthorne E, Janmey PA, Assoian RK: **Cell cycle control by physiological matrix elasticity and in vivo tissue stiffening**. *Curr. Biol.* 2009, **19**:1511–1518.
4. Pfeifer CR, Alvey CM, Irianto J, Discher DE: **Genome variation across cancers scales with tissue stiffness – An invasion-mutation mechanism and implications for immune cell infiltration**. *Curr. Opin. Syst. Biol.* 2017, **2**:102–113.
5. Irianto J, Xia Y, Pfeifer CR, Athirasala A, Ji J, Alvey C, Tewari M, Bennett RR, Harding SM, Liu AJ, et al.: **DNA damage follows repair factor depletion and portends genome variation in cancer cells after pore migration**. *Curr. Biol.* 2017, **27**:210–223.

Figure S1

—— Meta-analysis suggests that additional mechanisms—beyond replication errors—contribute to cancerous mutations ——

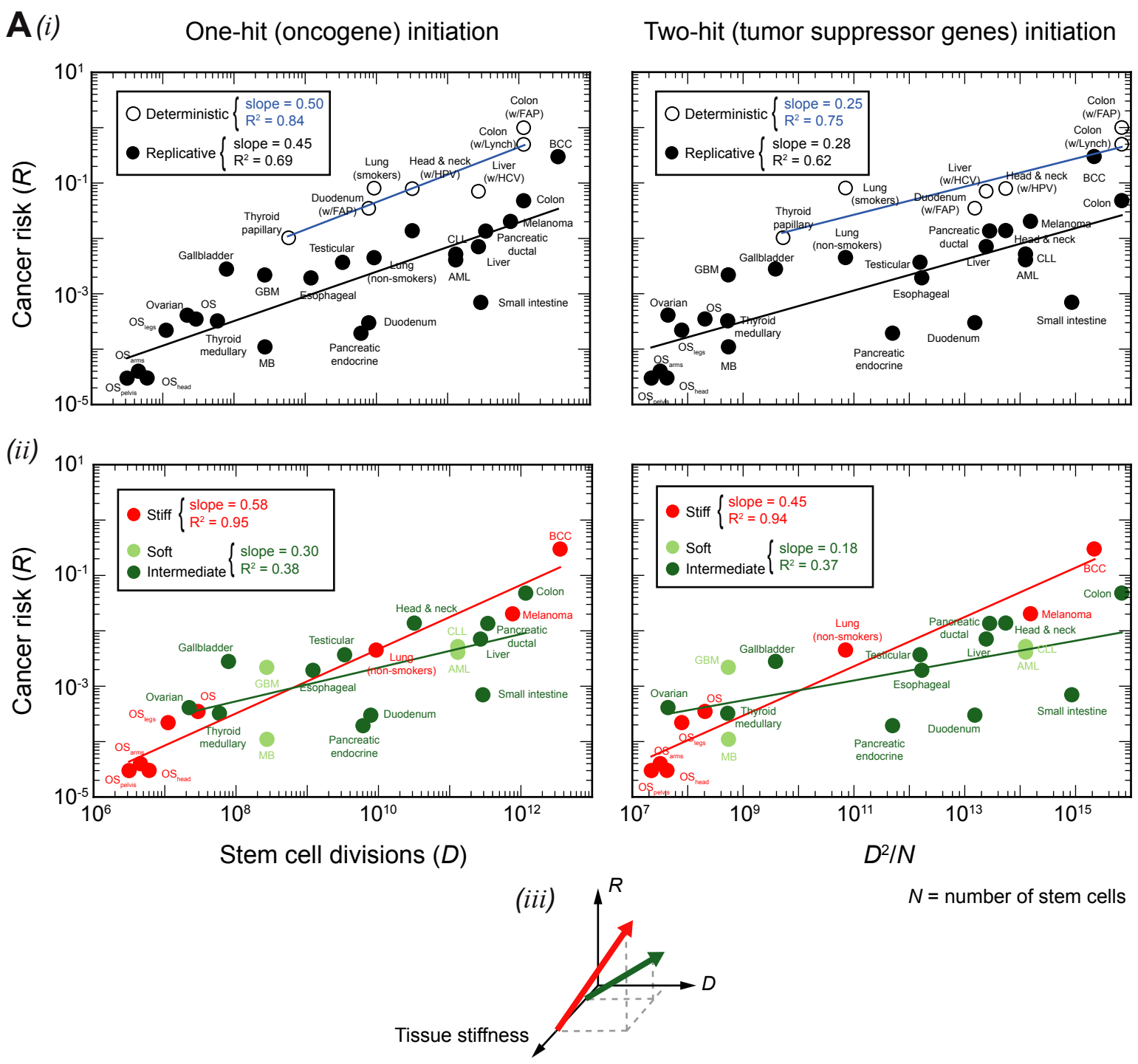

Under controlled pressure, lamin-B dilates per theoretical predictions and a repair factor leaks out of the nucleus without a bleb

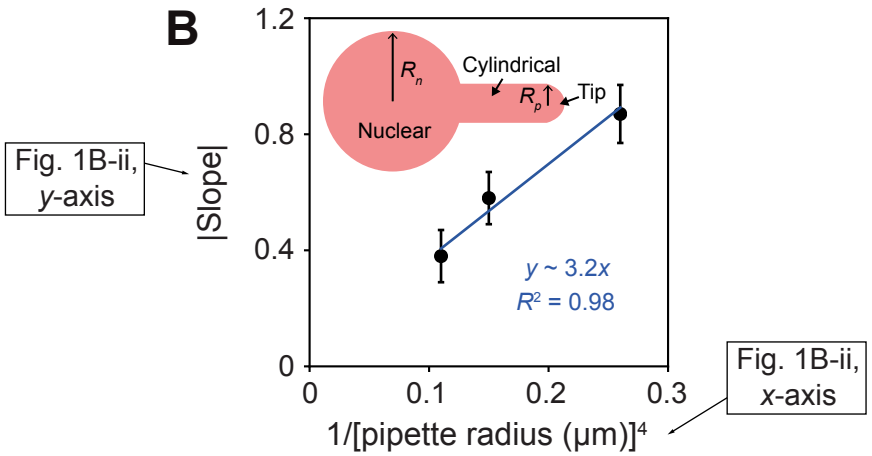

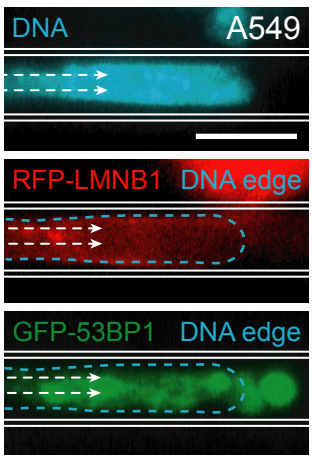

Figure S2

For three different cancer cell lines, γH2AX foci counts are suppressed in late cell cycle

A

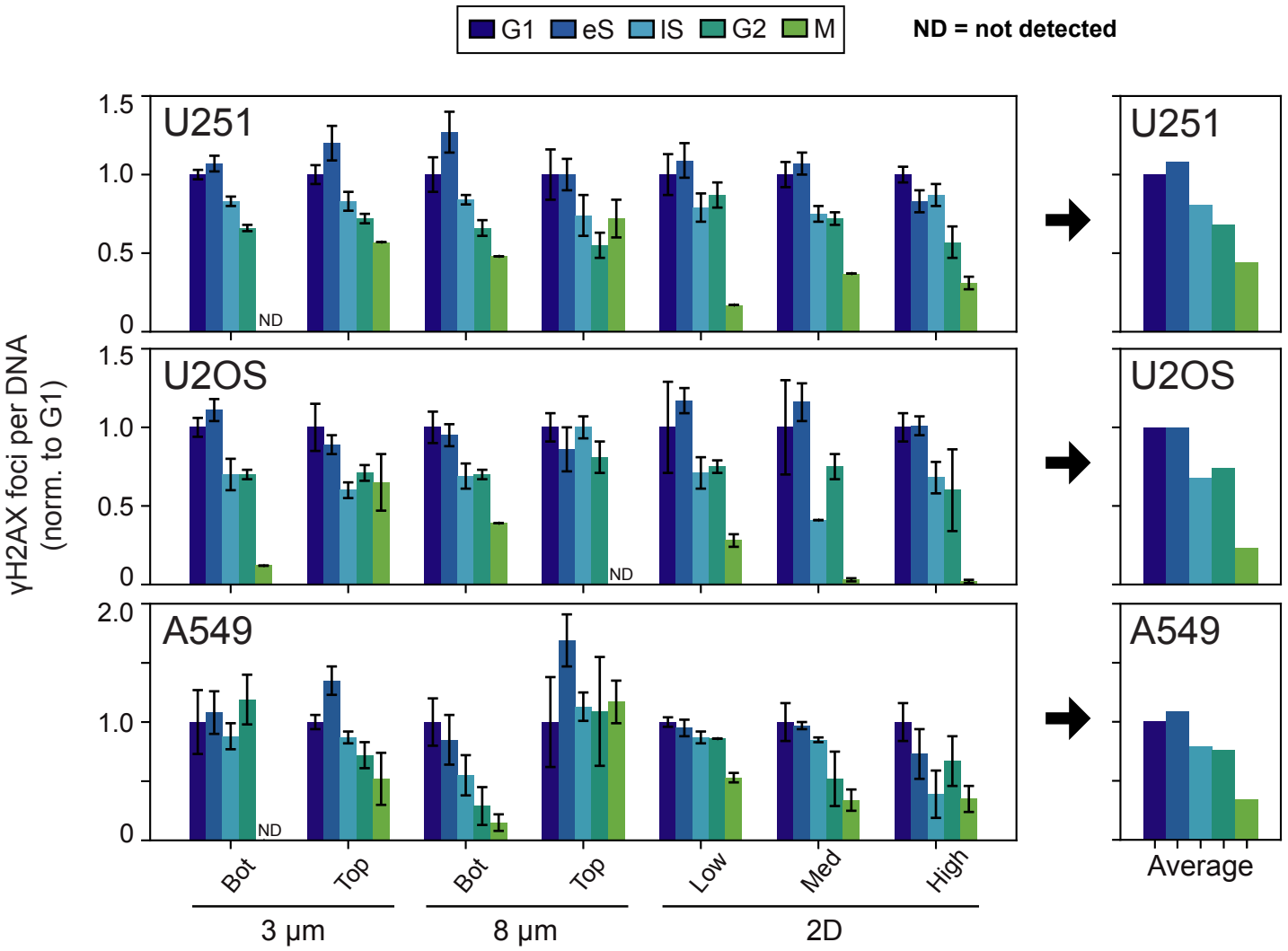

Trends suggest that constricting pores prevent entry into mitosis

B

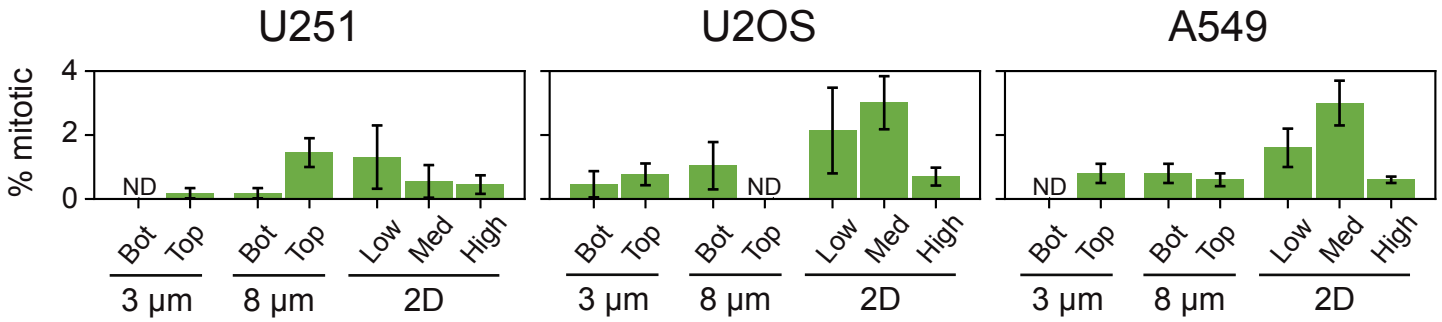

Figure S3

Averaging across multiple U2OS migration experiments confirms that constriction depletes 4N cells and increases DNA breaks

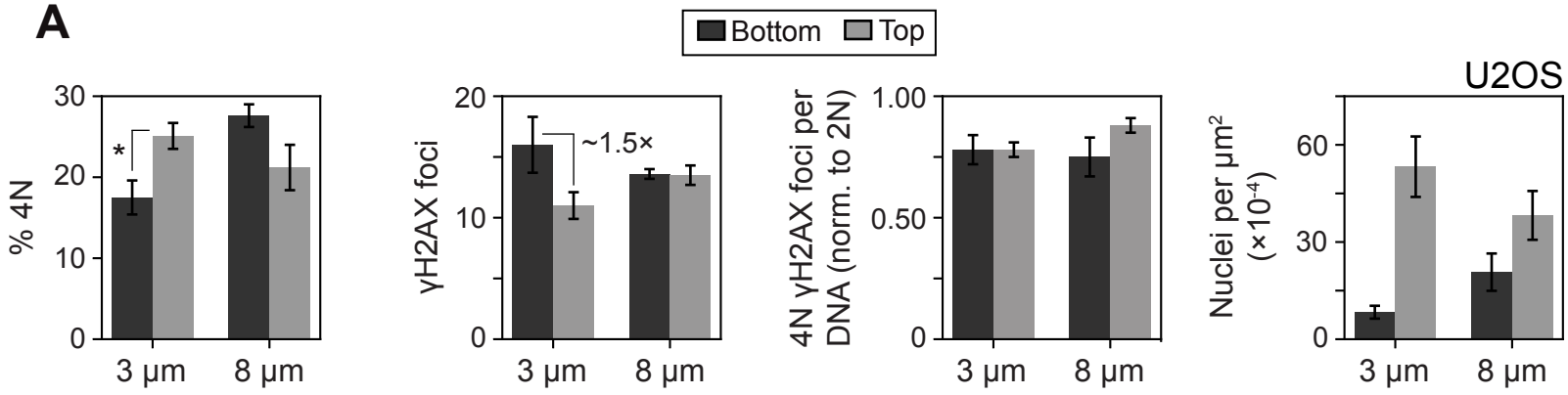

Excess BRCA1 foci after constricted migration can be explained by cell cycle perturbation

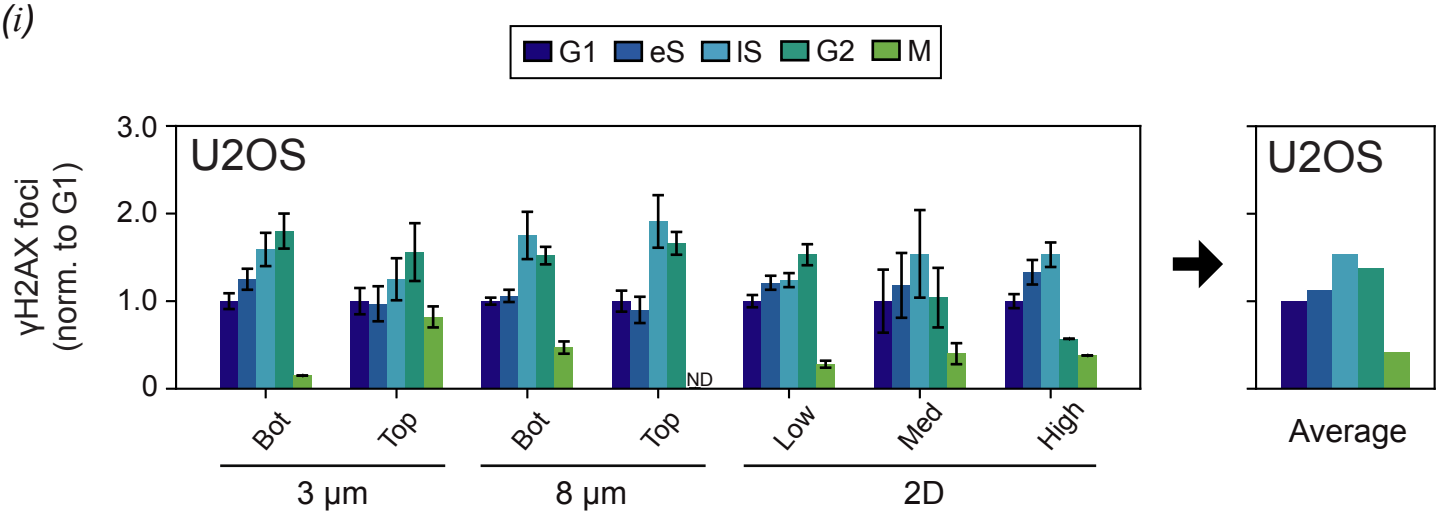

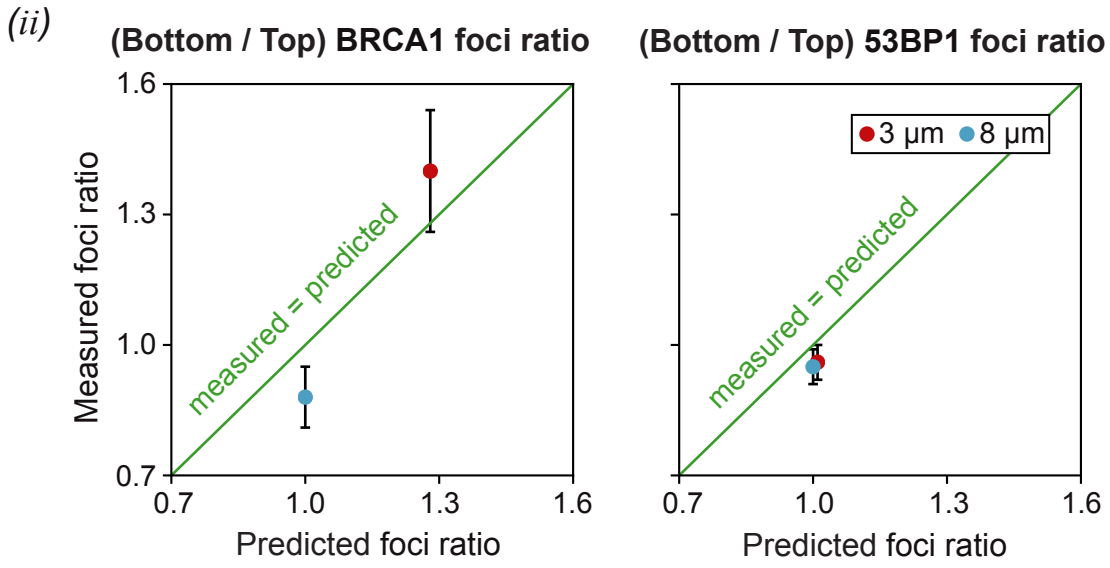

Figure S4

Partial knockdown of topoisomerase does not reduce constriction-induced DNA damage

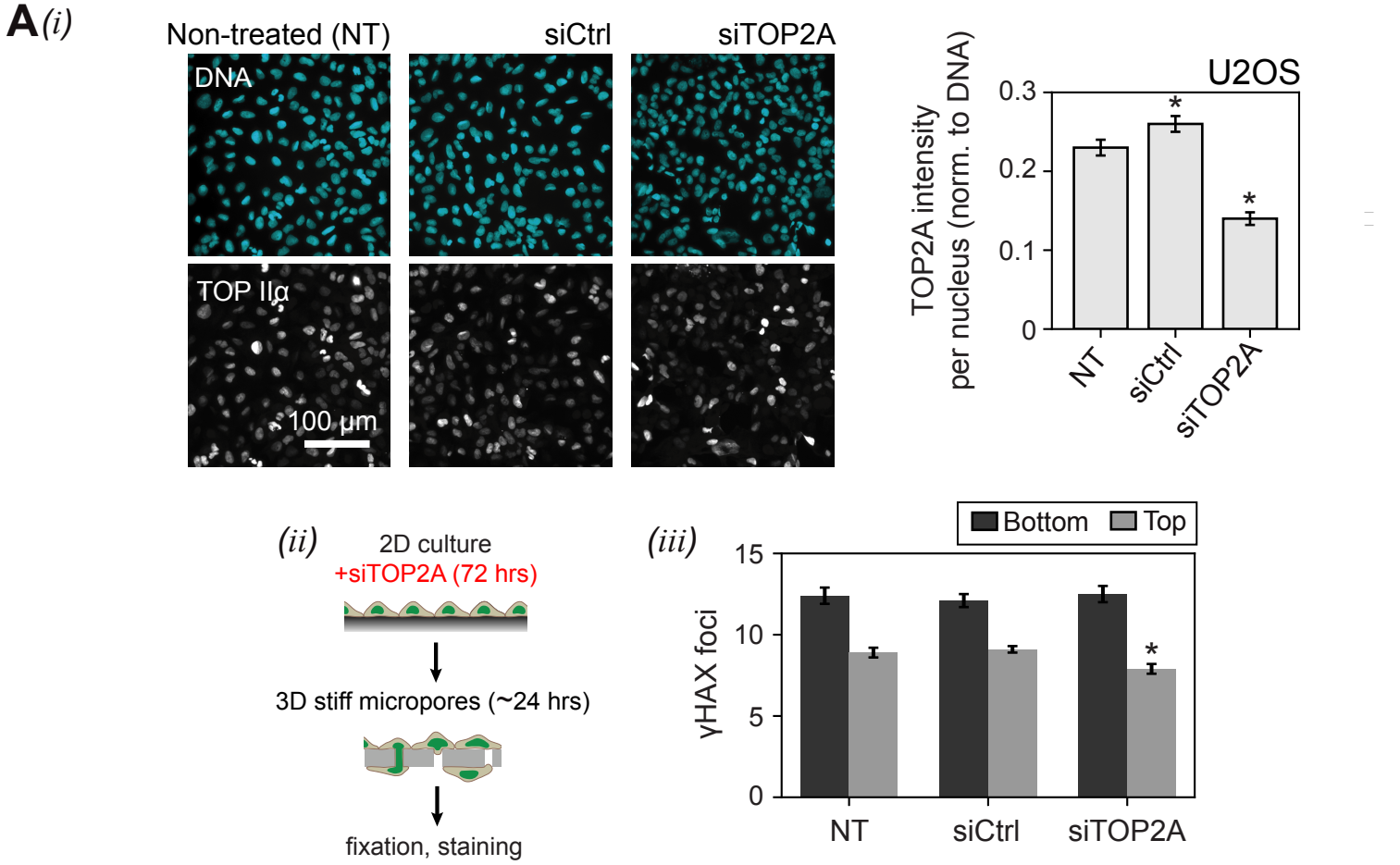

— Even with induction of DNA damage during S phase *via* etoposide treatment, 2N and 4N cells migrate through small pores —

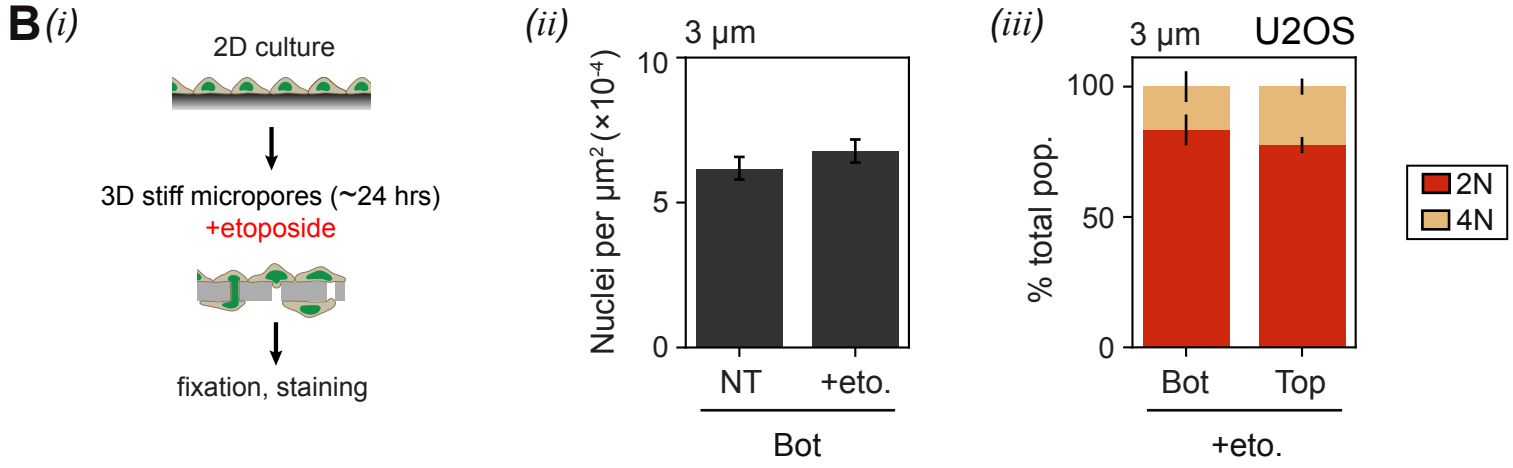

Figure S5

Treatment with PD, a CDK4/6 inhibitor, suppresses DNA synthesis and mitosis, effectively 'freezing' cells in G1 or G2

A

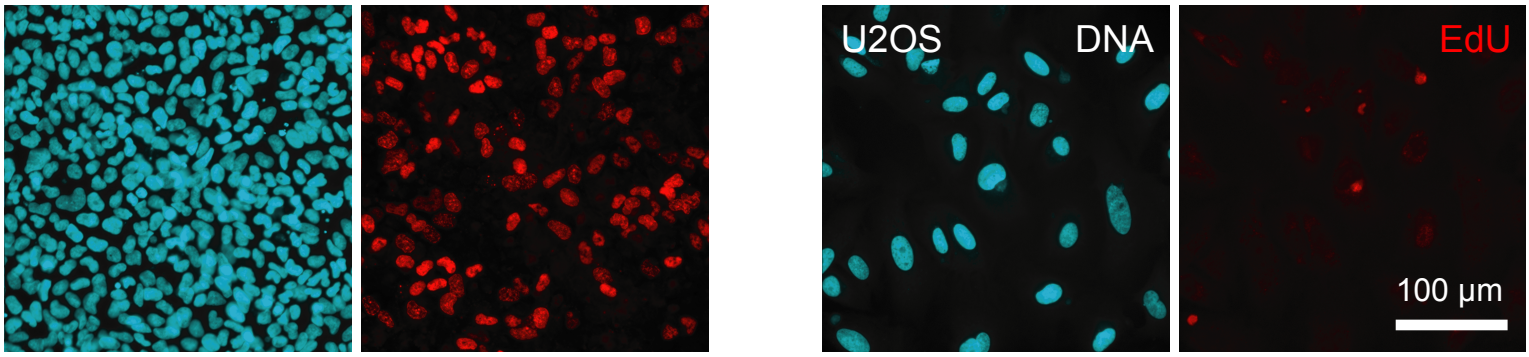

24.7 (± 1.5) % EdU-positive
0.8 (± 0.3) % mitotic

3.4 (± 0.3) % EdU-positive
0.2 (± 0.2) % mitotic

PD treatment yields a reduced cell density on the top and bottom of the Transwell membrane

B